Search for η_c' and study of χ_{cJ}

Yuan Changzheng
Institute of High Energy Physics,
Beijing 100039, P.R.China
E-mail: Yuancz@bepc5.ihep.ac.cn

Jun. 1997

Abstract

A data sample of 3.7 million ψ's, collected by BES operating at BEPC from 1993 to 1995, is used to search for the n=2 S-wave spin singlet charmonium state η_c' in ψ' radiative decays. Many of the all-charged-tracks decay modes of η_c' are tried, including $p\bar{p}$, $\pi^+\pi^-\pi^+\pi^-$, $\pi^+\pi^-K^+K^-$, $\pi^+\pi^-p\bar{p}$, $K^+K^-K^+K^-$, $K_s^0K^+\pi^- + c.c.$ and $3(\pi^+\pi^-)$. A 3.1σ and 2.1σ signal is seen in $\pi^+\pi^-K^+K^-$ and $3(\pi^+\pi^-)$ modes with mass around $3590 \sim 3600$MeV and width less than 10MeV at 90% confidence level. It looks very like the η_c' candidate reported by Crystal Ball collaboration. Its quantum number can not be determined from the limited statistics results in the ambiguity of whether it is η_c', but the characteristics of its resonance parameters, its formation and decay characteristics show that it is a very strong candidate of η_c'. The production rates of the signal in $\pi^+\pi^-K^+K^-$ and $3(\pi^+\pi^-)$ modes are determined to be $\mathcal{B}(\psi' \to \gamma X(3594)) \cdot \mathcal{B}(X(3594) \to \pi^+\pi^-K^+K^-) = (9.3 \pm 3.2 \pm 5.9) \times 10^{-5}$ and $\mathcal{B}(\psi' \to \gamma X(3594)) \cdot \mathcal{B}(X(3594) \to 3(\pi^+\pi^-)) = (7.7 \pm 4.2 \pm 4.2) \times 10^{-5}$ respectively; the upper limits of the production rates in other channels are also measured.

The P-wave spin triplet charmonium states $\chi_{cJ}(J = 0, 1, 2)$ are studied as the by-products of η_c' searching, $\chi_{c0} \to p\bar{p}$, $\chi_{c1} \to K_s^0K^+\pi^- + c.c.$, $\chi_{c0} \to K_s^0K_s^0$, $\chi_{c2} \to K_s^0K_s^0$, $\chi_{c0} \to \phi\phi$, $\chi_{c2} \to \phi\phi$ and $\chi_{cJ} \to K^+K^-K^+K^-$ are first observed and the corresponding branching fractions are determined; the branching fractions of all other decay channels are measured with high statistics, the mean values are changed significantly and the precision is improved compared to previous measurements.

1 Introduction

Of all the charmonium states below $D\bar{D}$ threshold, the n=2 S-wave spin singlet state η_c' and the P-wave spin singlet state $h_c(^1p_1)$ are the two states need confirmation, the P-wave spin triplet states χ_{cJ}, although many decay modes listed by PDG[1], most of the hadronic decays were measured in only one experiment based on 30,000 produced ψ's [2]. The observation of $h_c(^1p_1)$ at BES is not easy because it is produced in $\pi^0h_c(^1p_1)$ mode of ψ' decays with two low energy photons which is hard to detect at BES besides the low production rate, since $\psi' \to \pi^0h_c(^1p_1)$ violates isospin so it can not be produced via strong interaction. The searching for η_c' is a bit easier than detecting $h_c(^1p_1)$ since only one low energy photon need detection. The purpose of this analysis is then concentrated on searching for η_c' and measure the branching fractions of χ_{cJ} decays in corresponding final states.

The only candidate of η_c' was reported by Crystal Ball Collaboration in 1982 in their inclusive photon spectrum study [3]. The mass of the candidate is measured to be $m = 3594 \pm 5$MeV and the width $\Gamma < 8$MeV at 90% confidence level. E760 at Fermilab tried a $p\bar{p}$ scan in $3584 < \sqrt{s} < 3624$MeV range [4], but failed to find any compelling signal so the upper limits of $\mathcal{B}(\eta_c' \to p\bar{p}) \times (\eta_c' \to \gamma\gamma)$ as a function of ECM is given. E835, the upgrading version of E760, scheduled a more careful scan for η_c', no result reported yet.

According to the potential model and the measured parameters of other charmonium states, especially those of J/ψ and η_c, the resonance parameters of η_c' can be estimated. Following is the expectation of the so called "conventional wisdom".

1.1 Mass of η_c'

The mass split between S-wave spin triplet and spin singlet is caused by the spin-spin interaction part of the potential, namely

$$H_{HFS} = \frac{16\pi\alpha_s}{9m_c^2}\vec{S}_c \cdot \vec{S}_{\bar{c}}\delta^3(\vec{r}),$$

where m_c and $\vec{S}_c$ are the mass and spin vector of the charm quark respectively. The mass split between ψ' and η_c' is related to that between J/ψ and η_c in the following way:

$$\frac{\Delta M(\psi' - \eta_c')}{\Delta M(J/\psi - \eta_c)} \approx \frac{\alpha_s(\psi')}{\alpha_s J/\psi} \cdot \frac{|R_{2S}(0)|^2}{|R_{1S}(0)|^2},$$

where $R_{nS}(0)$ is the radial wave function of $c\bar{c}$ at origin, which can be estimated from the leptonic decay width of $\psi(nS)$,

$$\Gamma_{\psi(nS)\to e^+e^-} = \frac{16\pi}{3}\alpha^2 e_c^2 \frac{|R_{nS}(0)|^2}{m_{\psi(nS)}^2},$$

where $e_c = \frac{2}{3}$ is the charge of c-quark. Then one gets

$$m_{\psi'} - m_{\eta_c'} \approx \frac{\alpha_s(\psi')}{\alpha_s(J/\psi)} \cdot \frac{m_{\psi'}^2}{m_{J/\psi}^2} \cdot \frac{\Gamma_{\psi'\to e^+e^-}}{\Gamma_{J/\psi\to e^+e^-}} \cdot (m_{J/\psi} - m_{\eta_c}),$$

using corresponding data from PDG[1] and assuming $\frac{\alpha_s(\psi')}{\alpha_s(\eta_c')} = 0.9$, then

$$m_{\psi'} - m_{\eta_c'} \approx 65\text{MeV},$$

namely, $m_{\eta_c'} \approx 3621$MeV.

The mass of η_c' varys significantly (from 3589 to 3631MeV) in different potential models [5], from them, we can only draw the conclusion that the mass of η_c' is between the mass of χ_{c2} and that of ψ'.

1.2 Full width of η_c'

The decay modes of η_c' include $\eta_c\pi\pi$, ${}^1P_1\gamma$, $J/\psi\gamma$ and light hadron final states (two gluons final states), namely,

$$\Gamma_{tot}(\eta_c') = \Gamma(\eta_c\pi\pi) + \Gamma({}^1P_1\gamma) + \Gamma(J/\psi\gamma) + \Gamma(gg).$$

It is estimated that $\Gamma(\eta_c\pi\pi) \approx 140$keV, the partial width of E1 transition $\Gamma(\eta_c' \to^1 P_1\gamma)$ is about 10keV and that of M1 transition $\Gamma(\eta_c' \to J/\psi\gamma)$ is 1keV [6]. The partial width of $\eta_c' \to gg$ is estimated from

$$\frac{\Gamma(\eta_c' \to gg)}{\Gamma(\eta_c \to gg)} \approx \frac{\Gamma(\psi' \to e^+e^-)}{\Gamma(J/\psi \to e^+e^-)},$$

so $\Gamma_{tot}(\eta_c') \approx \Gamma(\eta_c' \to gg) \approx 5$MeV.

1.3 Partial width of η_c'

In section 1.2, it is obvious that the main decay modes of η_c' is two gluons final states which is very like the η_c, so

$$\frac{\mathcal{B}(\eta_c' \to h)}{\mathcal{B}(\eta_c \to h)} \approx 1,$$

where h denotes the inclusive light hadron decay final states. Assuming the decay modes of η_c' is the same as that of η_c decays, one expect the same branching fractions of η_c' and η_c decays to the same exclusive decay channel. This is used in the summary of this paper to check whether the signal we observed is the η_c'.

1.4 Production rate of η_c' in ψ' decays

η_c' is produced in ψ' decays by M1 transition, in the non-relativistic limit, the transition amplitude is the same as that of $J/\psi \to \gamma\eta_c$, so

$$\mathcal{B}(\psi' \to \gamma\eta_c') = \frac{\Gamma(J/\psi \to \gamma\eta_c)}{\Gamma_{tot}(\psi')} \cdot (\frac{k_{\eta_c'}}{k_{\eta_c}})^3,$$

where k_{η_c} and $k_{\eta_c'}$ are the momenta of η_c and η_c' in J/ψ and ψ' decay respectively.

Using the values given by PDG [1] and assuming the mass of η_c' equals the mass of CBAL η_c' candidate, $m_{\eta_c'} = 3594$MeV, one gets

$$\mathcal{B}(\psi' \to \gamma\eta_c') \approx 2 \times 10^{-3}.$$

Since $\mathcal{B}(\psi' \to \gamma\eta_c')$ proportional to the third power of $k_{\eta_c'}$, it decrease very quick as the mass of η_c' increase, assuming $m_{\eta_c'} = 3621$MeV, $\mathcal{B}(\psi' \to \gamma\eta_c')$ becomes 7×10^{-4}.

2 Events selection

2.1 Data sample

The data sample used in this analysis was taken by BES at BEPC in 1993/94 and 1995 runs, the total produced ψ' events is $3.7(1 \pm 10\%) \times 10^6$ calculated with inclusive $\psi' \to \pi^+\pi^- J/\psi$ events.

To eliminate the data sample, the following criteria are used for the two-prong, four-prong and six-prong events sample selection.

1. The number of charged tracks is required to be two, four or six with net charge zero and each track with high quality in track fitting(MFIT=2,-19 or -9);
2. Transverse momentum of each track $P_{xy} > 0.07\text{GeV}/c$;
3. $|\cos\theta_{MDC}| < 0.8$;
4. $0 < NNEU < 9$.

2.2 Charged tracks identification

Using the frame of D_s official partid program—PARTID1 with TOF and dE/dx correction parameters got from two ψ' data sets. A correction of the deviations of dE/dx XS is introduced instead of using the default value of one for D_s data. The Monte Carlo simulated data is treated in different way and with different correction parameters. The codes are checked with $\psi' \to \pi^+\pi^- J/\psi$, $J/\psi \to \rho\pi$, the partid probability of the tracks in different momentum range distributes uniformly between zero and one as expected.

2.3 γ selection

A neutral cluster is regarded as a photon candidate when the angle in xy plane between the nearest charged track and the cluster greater than 15^0, the first layer of the hit not in the sixth layer of BSC, and the cosine of the angle between cluster develop direction and its emit direction greater than 0.80. When these selection criteria used to select γ candidates in $\psi' \to \pi^+\pi^-\pi^+\pi^-$ and $\psi' \to \pi^+\pi^- K^+K^-$, less than 20% events can find γ's.

2.4 K_s^0 finding—$K_s^0 K^\pm \pi^\mp$ channel only

Of every two charged tracks with net charge zero and effective mass lies between $M_{K^0} - 0.200$ and $M_{K^0} + 0.200$ when they are assumed to be π, the combination with mass most near K_s^0 nominal energy is considered to be K_s candidate, the number of combinations in the event is counted as NKSHORT. K_s vertex is got by crossing these two tracks and the primary vertex is estimated with the cross point of another two charged tracks assuming one of them is kaon and another pion. Two parameters are defined to identify the K_s: the distance between primary vertex and secondary vertex in $R-\phi$ plain L_{xy} and the cosine of the angle between the K_s momentum and its vertex direction $CSKS$ which is expected to be very near one for a real K_s event.

2.5 Events selection criteria

For all the channels we studied, the four constraints kinematics fit probability is required to be greater than 1%, the probabilities of PARTID of each charged tracks greater than 1%.

To remove the contamination from $\psi' \to \pi^+\pi^- J/\psi$, the total momentum of every two different charged tracks is needed to be greater than 650MeV, this remove all this kind of events.

At most four selected gamma candidates are allowed in each event, we use four to eliminate the difference between data and Monte Carlo, the later cannot simulated enough fake photons.

2.5.1 $\gamma\pi^+\pi^-\pi^+\pi^-$ and $\gamma\pi^+\pi^-K^+K^-$

A combined probability of the four-constraint kinematics fit and particle identification

$$proball = prob4c \cdot prbid^+_{p_h} \cdot prbid^+_{p_l} \cdot prbid^-_{p_h} \cdot prbid^-_{p_l}$$

is used to separate $\gamma\pi^+\pi^-\pi^+\pi^-$ and different combinations of $\gamma\pi^+\pi^-K^+K^-$ assumption.

To select $\gamma K^0_s K^0_s$ events, the mass of one combination of $\pi^+\pi^-$ and another combination should lies in a 2σ region around K^0_s nominal mass.

2.5.2 $\gamma\pi^+\pi^-p\bar{p}$

If one of the four tracks is identified as proton or antiproton the event is assumed to be $\gamma\pi^+\pi^-p\bar{p}$.

2.5.3 $\gamma K^+K^-K^+K^-$

To select $\phi\phi$ events, we requires the mass of the K^+K^- ranges from 0.99 to 1.05GeV, this is estimated from a fitting to the data, which gives mass equals 1.023 ± 0.001GeV and sigma equals 0.0085 ± 0.0011GeV when fitted with a gaussian.

2.5.4 $\gamma K^0_s K^+\pi^- + c.c.$

Number of K^0_s candidate NKSHORT equals one, L_{xy} greater than 5mm and CSKS greater than 0.98, the mass of K^0_s candidate after 4C-fit lies in 2σ around K^0_s nominal mass.

2.5.5 $\gamma 3(\pi^+\pi^-)$

To remove the contamination from $\psi' \to \pi^+\pi^- J/\psi$ to total momentum of the lowest momentum positive charged track and negative charged track is needed to be greater than 550MeV instead of using 650MeV used in other modes.

2.5.6 $\gamma p\bar{p}$

1. Both tracks must have $prob_p > 0.05$ and at least one track has $prob_p > prob_\pi$ and $prob_p > prob_K$.

2. Do 4C-fit to $\psi' \to \gamma p\bar{p}$ to the two charged tracks and the gamma candidates with largest SC energy, the χ^2 probability of the fit is required to be greater than 5%.

3 Monte Carlo

The angular distribution of $\psi' \to \gamma X$ is simulated assuming pure E1 transition, namely $1+\cos^2\theta$, $1-\frac{1}{3}\cos^2\theta$ and $1+\frac{1}{13}\cos^2\theta$ for the spin of X resonance $J=0,1$ and 2 respectively in laboratory system. The X (χ_{cJ} or η_c') and $K_s^0 \to \pi^+\pi^-$, $\phi \to K^+K^-$ decays are simulated according to phase space distribution. 10000 events are simulated for each decay channel with V86, V154 and reconstructed with V86.

4 Systematic error

Including the error of varying cuts, errors of $B(\psi' \to \gamma\chi_{cJ})$ and $B(K_s^0 \to \pi^+\pi^-)$ or $B(\phi \to K^+K^-)$, the uncertainty of ψ' events number and the limited statistics of Monte Carlo simulated events.

5 Results

5.1 Branching fractions

5.1.1 $\pi^+\pi^-\pi^+\pi^-$ mode

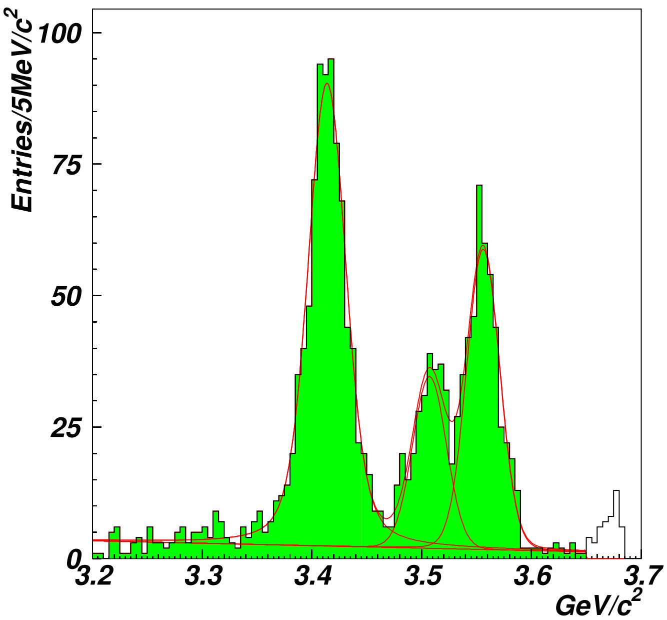

Figure 1: Fitted results of the $\pi^+\pi^-\pi^+\pi^-$ mass plots. Mass resolutions are fixed to Monte Carlo values, widths of χ_{c1} and χ_{c2} are fixed to PDG values.

	χ_{c0}	χ_{c1}	χ_{c2}
events number	854.7 ± 28.5	254.2 ± 18.5	439.1 ± 21.3
resolution(MeV)	14.31	15.21	14.61
efficiency	15.88%	16.54%	15.01%
$B(\chi_{cJ} \to \pi^+\pi^-\pi^+\pi^-)(\times 10^{-3})$	$15.64 \pm 0.52 \pm 2.35$	$4.77 \pm 0.35 \pm 0.78$	$10.14 \pm 0.49 \pm 1.59$

5.1.2 $K_s^0 K_s^0$ mode

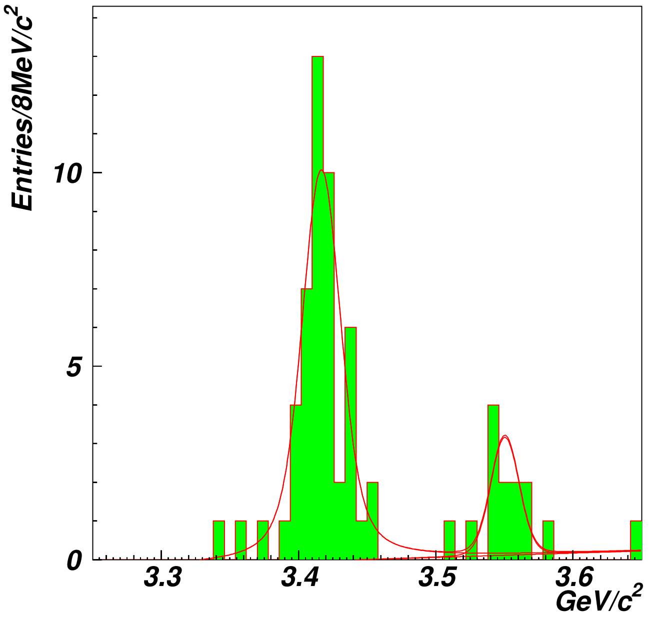

Figure 2: Fitted results of the $K_s^0 K_s^0$ mass plots. Mass resolutions are fixed to Monte Carlo values, width of χ_{c2} is fixed to PDG value.

	χ_{c0}	χ_{c2}
events number	53.8 ± 3.3	9.1 ± 3.3
resolution(MeV)	10.84	9.87
efficiency	13.93%	13.83%
$B(\chi_{cJ} \to K_s^0 K_s^0)(\times 10^{-3})$	$2.39 \pm 0.14 \pm 0.41$	$0.48 \pm 0.17 \pm 0.10$

5.1.3 $\pi^+\pi^- K^+ K^-$ mode

	χ_{c0}	χ_{c1}	χ_{c2}
events number	566.7 ± 26.0	181.0 ± 14.6	252.0 ± 16.4
resolution(MeV)	15.94	14.74	15.09
efficiency	11.60%	12.28%	11.02%
$B(\chi_{cJ} \to \pi^+\pi^- K^+ K^-)(\times 10^{-3})$	$14.20 \pm 0.65 \pm 2.67$	$4.58 \pm 0.37 \pm 0.87$	$7.92 \pm 0.52 \pm 1.61$

5.1.4 $\pi^+\pi^- p\bar{p}$ mode

	χ_{c0}	χ_{c1}	χ_{c2}
events number	69.3 ± 9.9	16.9 ± 6.2	49.4 ± 8.0
resolution(MeV)	12.87	13.90	13.86
efficiency	12.63%	14.86%	13.39%
$B(\chi_{cJ} \to \pi^+\pi^- p\bar{p})(\times 10^{-3})$	$1.60 \pm 0.23 \pm 0.39$	$0.35 \pm 0.13 \pm 0.12$	$1.28 \pm 0.21 \pm 0.32$

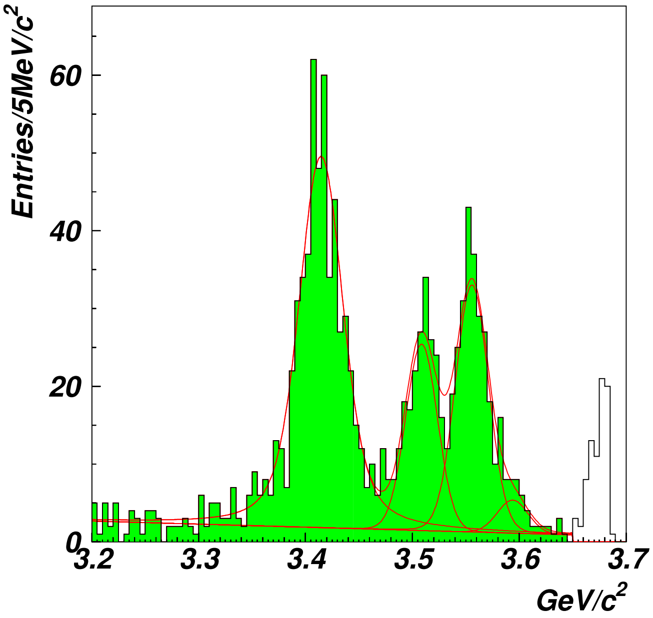

Figure 3: Fitted results of the $\pi^+\pi^-K^+K^-$ mass plots. Mass resolutions are fixed to Monte Carlo values, widths of χ_{c1} and χ_{c2} are fixed to PDG values. Fitted together with a Breit-Wigner at (3593.9 ± 5.4)MeV, the possible η_c', events number is (30.7 ± 10.6), signal significance is 3.1σ. Production rate $B(\psi' \to \gamma\eta_c') \times B(\eta_c' \to \pi^+\pi^-K^+K^-) = (9.3 \pm 3.2) \times 10^{-5}$, efficiency is 0.0895 and mass resolution is 14.42MeV.

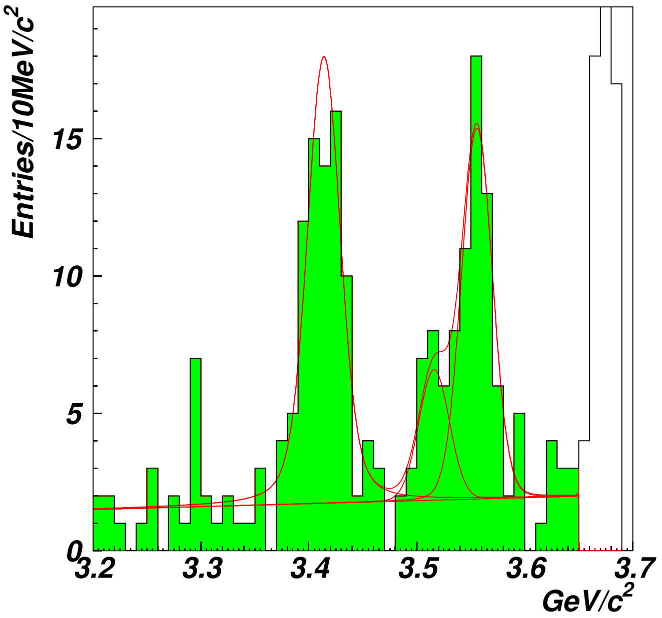

Figure 4: Fitted results of the $\pi^+\pi^-p\bar{p}$ mass plots. Mass resolutions are fixed to Monte Carlo values, widths of χ_{c1} and χ_{c2} are fixed to PDG values.

5.1.5 $K^+K^-K^+K^-$ mode

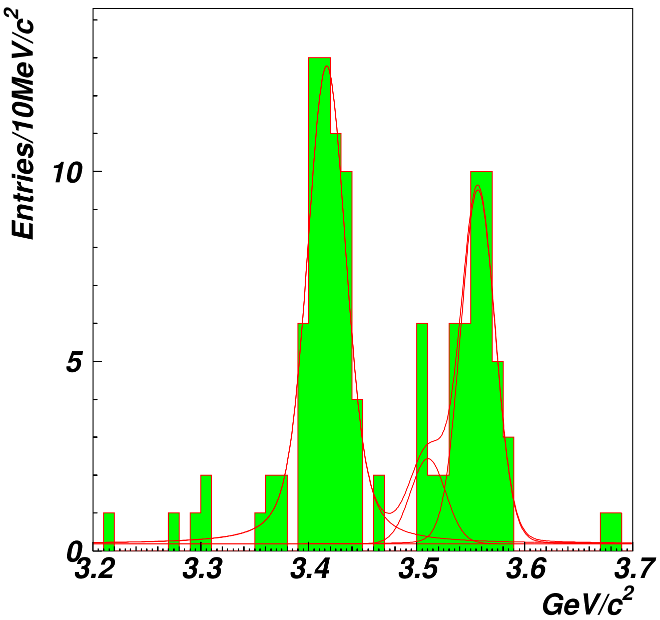

Figure 5: Fitted results of the $K^+K^-K^+K^-$ mass plots. Mass resolutions are fixed to Monte Carlo values, widths of χ_{c1} and χ_{c2} are fixed to PDG values.

	χ_{c0}	χ_{c1}	χ_{c2}
events number	64.4 ± 6.3	9.2 ± 3.9	37.9 ± 5.7
resolution(MeV)	14.3	16.1	15.4
efficiency	6.94%	7.62%	8.00%
B($\chi_c \to K^+K^-K^+K^-$)($\times 10^{-3}$)	$2.70 \pm 0.26 \pm 0.46$	$0.38 \pm 0.16 \pm 0.12$	$1.64 \pm 0.25 \pm 0.31$

5.1.6 $\phi\phi$ mode

	χ_{c0}	χ_{c1}	χ_{c2}
events number	6.6 ± 2.4	< 3.89	12.5 ± 2.4
resolution(MeV)	11.0	9.41	10.1
efficiency(%)	9.64	10.26	9.86
B($\chi_c \to \phi\phi$)($\times 10^{-3}$)	$0.83 \pm 0.30 \pm 0.22$	< 0.49	$1.82 \pm 0.35 \pm 0.44$

5.1.7 $K_s^0 K^+ \pi^- + c.c.$ mode

	χ_{c0}	χ_{c1}	χ_{c2}
events number	< 10	31 ± 6	< 14
resolution(MeV)	13.60	13.80	13.73
efficiency	5.11%	5.74%	5.33%
B($\chi_{cJ} \to K_s^0 K^+ \pi^- + c.c.$)($\times 10^{-3}$)	< 0.83	$2.45 \pm 0.47 \pm 0.52$	< 1.3

5.1.8 $3(\pi^+\pi^-)$ mode

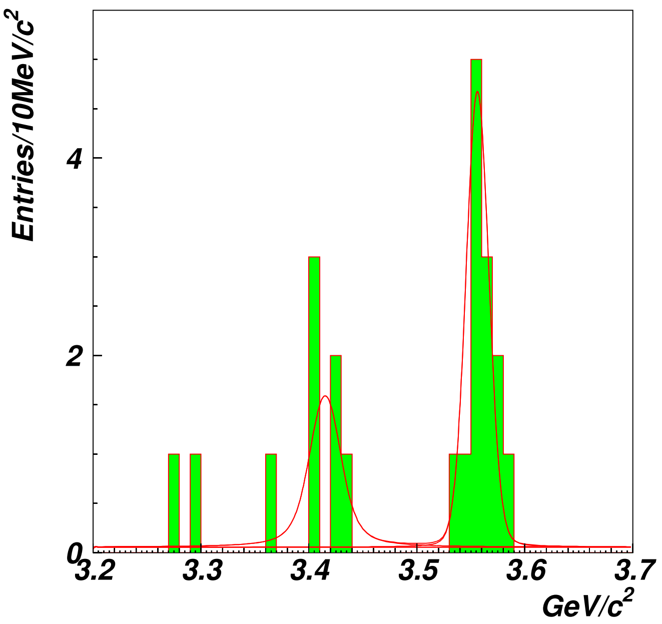

Figure 6: Fitted results of the $\phi\phi$ mass plots, Mass resolutions are fixed to Monte Carlo values, width of χ_{c0} is fixed to 15.0MeV and that of χ_{c2} is fixed to PDG value.

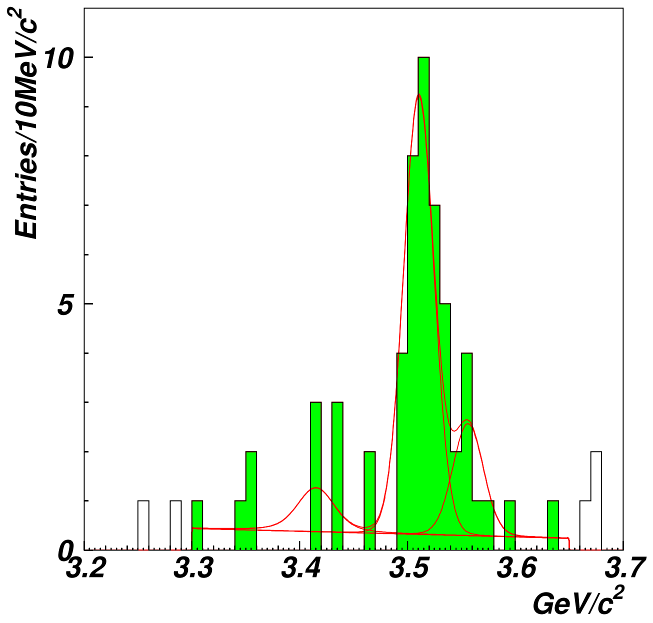

Figure 7: Fitted results of the $K_s^0 K^+ \pi^- + c.c.$ mass plots. Resolutions are fixed to Monte Carlo value, mass and width of χ_{c1} and χ_{c2} mass of χ_{c0} are fixed to PDG value and width of χ_{c0} is fixed to 15.0MeV.

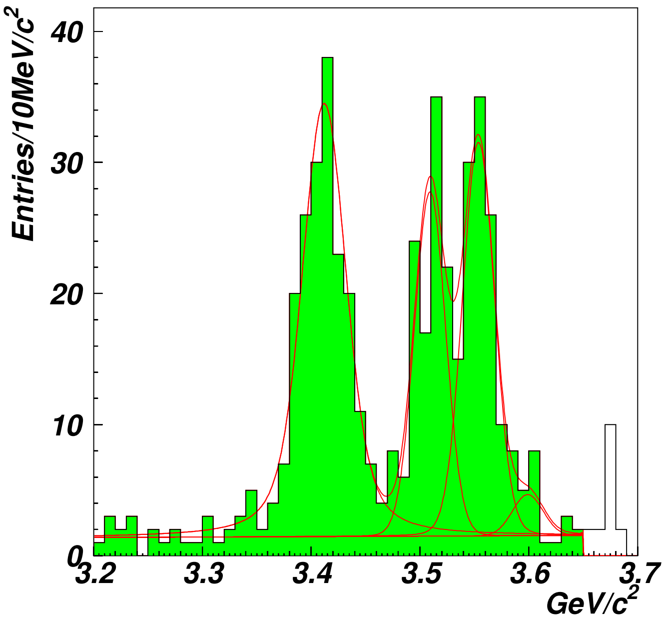

Figure 8: Fitted results of the $3(\pi^+\pi^-)$ mass plots. Mass resolutions are fixed to Monte Carlo values, widths of χ_{c1} and χ_{c2} are fixed to PDG values. Fitted together with a Breit-Wigner at (3598.7 ± 12.7)MeV, the possible η_c' with signal significance 2.1σ. Production rate $B(\psi' \to \gamma\eta_c') \times B(\eta_c' \to 3(\pi^+\pi^-)) = (7.7 \pm 5.9) \times 10^{-5}$.

	χ_{c0}	χ_{c1}	χ_{c2}
events number	191.6 ± 15.5	95.0 ± 11.0	112.6 ± 11.7
resolution(MeV)	15.76	14.17	14.28
efficiency	4.41%	5.12%	4.27%
$\mathrm{B}(\chi_{cJ} \to 3(\pi^+\pi^-))(\times 10^{-3})$	12.62 ± 1.02	5.76 ± 0.67	9.13 ± 0.95

5.1.9 $p\bar{p}$ mode

	χ_{c0}	χ_{c1}	χ_{c2}
Events number	16.4 ± 4.2	6.8 ± 3.0	7.9 ± 3.1
Mass resolution(MeV)	6.2	7.2	6.8
Detection efficiency (%)	33.0	35.9	32.0
$\mathcal{B}(\chi_{cJ} \to p\bar{p})(\times 10^{-5})$	$14.4 \pm 3.7 \pm 3.1$	$5.9 \pm 2.6 \pm 1.9$	$8.6 \pm 3.4 \pm 3.7$

5.1.10 Summary

Table 1 summarize the branching fractions of χ_{cJ} decays, previous measurements used by PDG to evaluate the world average is also listed. From the table we can see some new decay modes are observed and branching fractions are measured, and some other channels, branching fractions with high precision are given. It is notable that the branching fractions got from this analysis give a lower value compared with the values listed by PDG (typically a factor of 1/2 lower than PDG values).

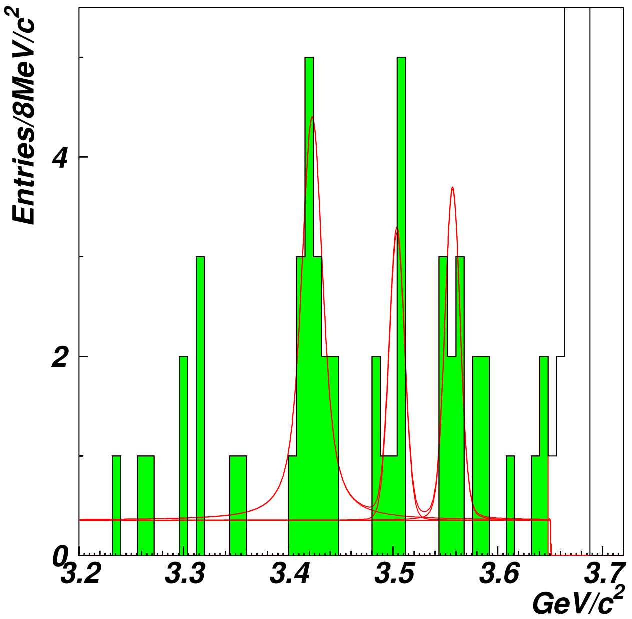

Figure 9: $p\bar{p}$ invariant mass of $\gamma p\bar{p}$ events. Mass resolutions are fixed to Monte Carlo values, masses and widths of χ_c are fixed to PDG values.

5.2 η_c' production

There is an obvious shoulder on the right side of $\pi^+\pi^-K^+K^-$ invariant mass distribution, assuming it is the expected η_c', fix the mass resolution to Monte Carlo value, we get the mass is (3593.9 ± 8.0)MeV with events number (30.7 ± 10.6), signal significance is 3.1σ. Production rate $B(\psi' \to \gamma\eta_c') \times B(\eta_c' \to \pi^+\pi^-K^+K^-) = (9.3 \pm 3.2 \pm 5.9) \times 10^{-5}$. If we free the mass resolution, the fit leads to mass equals to (3595.0 ± 3.6)MeV, events number (23.0 ± 8.9) and significance 3.3σ. This result consistent with that when mass resolution fixed. Current knowledge about this signal can not allow us determine its width, instead, the fit gives an upper limit of 10MeV at 90% C.L..

Backgrounds from $\psi' \to \gamma\chi_c \to \gamma K_s^0 K^\pm\pi^\mp \to \gamma\pi^+\pi^-K^\pm\pi^\mp$ do not lies around 3594MeV, and negligible, see fig. 10; backgrounds from $\psi' \to \gamma\chi_c \to \gamma\pi^+\pi^-\pi^+\pi^-$ are very small compared to the signals in $\pi^+\pi^-K^+K^-$ mode, see fig. 11, according to our Monte Carlo study. Backgrounds from $\psi' \to \pi^0\pi^+\pi^-\pi^+\pi^-$ or $\pi^0\pi^+\pi^-K^+K^-$ are also negligible in the mass region we interested in, and fig. 12 shows the mass distribution when we requiring only one gamma candidate in the event, the background level is very low, but the bump at 3594MeV still exist, which indicates the bump is not caused by these kinds of background. The clearly seen peaks at 3680MeV in the mass plots (figs. 1,3,4) are obvious ψ', with a misidentified low energy photon candidate, the appearance of this peak shows that the bump at 3594MeV is not caused by misidentified ψ' direct decays without gamma.

A 2.1σ signal is observed at mass (3598.7 ± 12.7)MeV, if it is the same signal as we seen in $\psi' \to \gamma\pi^+\pi^-K^+K^-$ mode, and assuming it is η_c', the production rate is $B(\psi' \to \gamma\eta_c' \to \gamma 3(\pi^+\pi^-)) = (7.7 \pm 4.2 \pm 4.2) \times 10^{-5}$.

The signal at (3598.7 ± 12.7)MeV in this channel is only 2.1σ, this cannot be a strong evidence of declaring a signal, but we checked the events in this mass region and found that

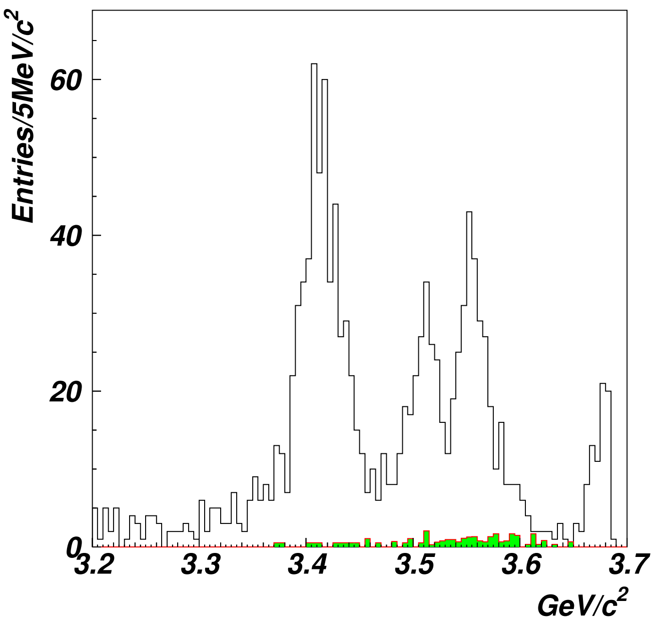

Figure 10: Shaded region is the backgrounds from $\chi_c \to \pi^+\pi^-\pi^+\pi^-$, normalized to produced events number estimated from this paper.

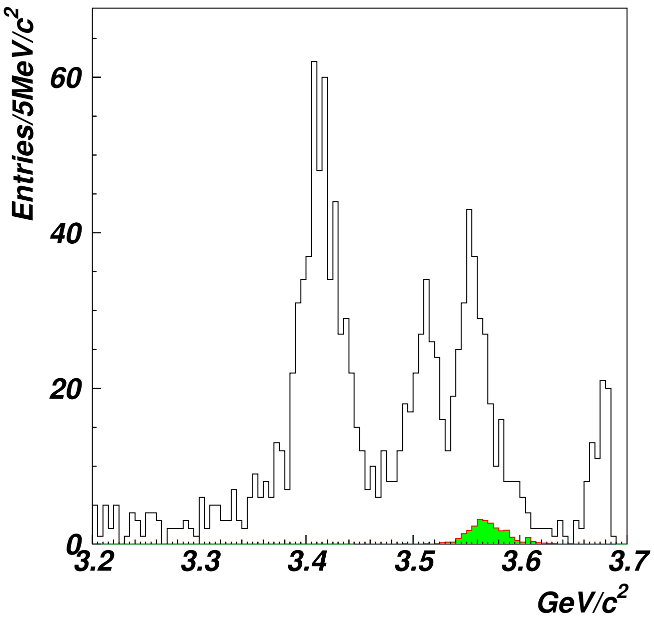

Figure 11: Shaded region is the backgrounds from $\chi_{c2} \to K_s^0 K^\pm \pi^\mp$, branching ratio of $\chi_{c2} \to K_s^0 K^\pm \pi^\mp$ using T.Himel's upper limit 2.1×10^{-3}, 50% larger than measured in this paper.

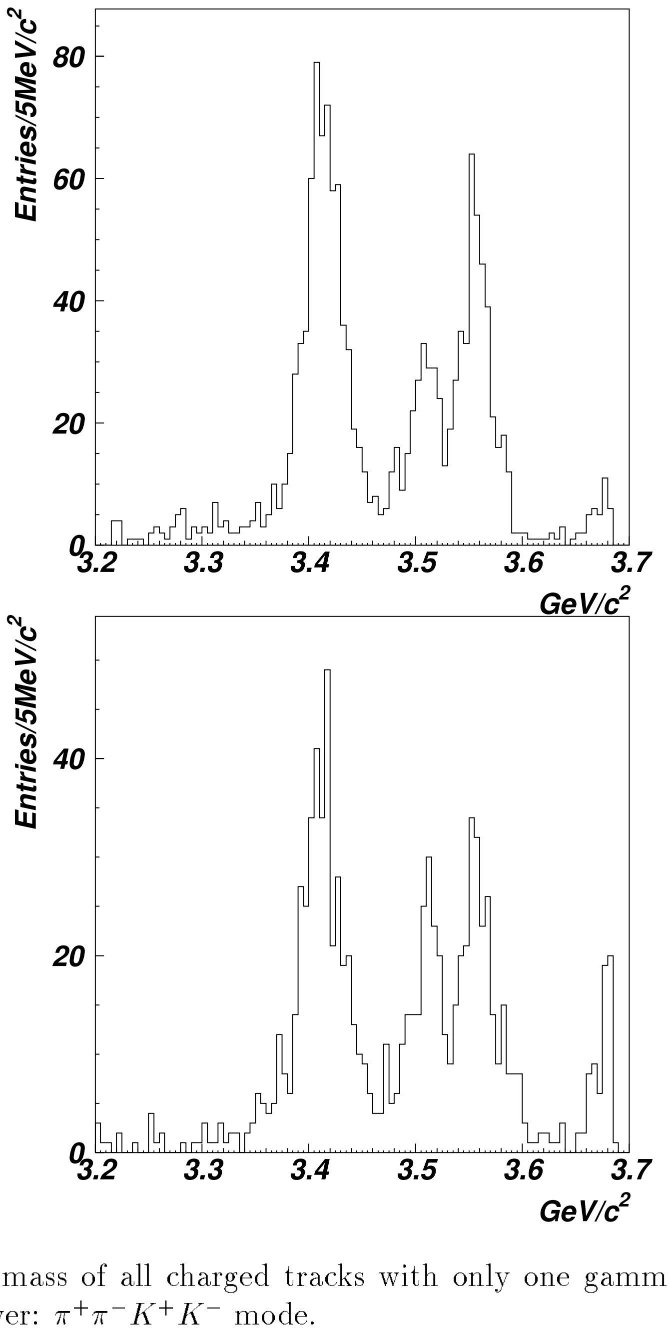

Figure 12: Invariant mass of all charged tracks with only one gamma candidate. Upper: $\pi^+\pi^-\pi^+\pi^-$ mode; lower: $\pi^+\pi^-K^+K^-$ mode.

Table 1: BES χ_{cJ} Results

	BES		PDG 96		
	evts number	result	evts number	World average	Reference
$\Gamma_{\chi_{c0}}$	350 ± 19	$15.0^{+3.2}_{-2.8}$ MeV	–	$13.5 \pm 3.3 \pm 4.2$MeV	[9]
$\mathcal{B}(\chi_{c0} \to \pi^+\pi^-)$	350 ± 19	$(4.27 \pm 0.23 \pm 0.60) \times 10^{-3}$	11	$(7.5 \pm 2.1) \times 10^{-3}$	[10]
			32 ± 6		[2]
$\mathcal{B}(\chi_{c2} \to \pi^+\pi^-)$	84 ± 9	$(1.52 \pm 0.17 \pm 0.29) \times 10^{-3}$	4	$(1.9 \pm 1.0) \times 10^{-3}$	[10]
$\mathcal{B}(\chi_{c0} \to K^+K^-)$	258 ± 16	$(3.44 \pm 0.21 \pm 0.47) \times 10^{-3}$	6	$(7.1 \pm 2.4) \times 10^{-3}$	[10]
			27 ± 5.5		[2]
$\mathcal{B}(\chi_{c2} \to K^+K^-)$	24 ± 5	$(0.52 \pm 0.11 \pm 0.18) \times 10^{-3}$	2	$(1.5 \pm 1.1) \times 10^{-3}$	[10]
$\mathcal{B}(\chi_{c0} \to p\bar{p})$	16.4 ± 4.2	$(14.4 \pm 3.7 \pm 3.1) \times 10^{-5}$		$< 9.0 \times 10^{-4}$	[10]
$\mathcal{B}(\chi_{c1} \to p\bar{p})$	6.8 ± 3.0	$(5.9 \pm 2.6 \pm 1.9) \times 10^{-5}$	513	$(8.6 \pm 1.2) \times 10^{-5}$	[7]
$\mathcal{B}(\chi_{c2} \to p\bar{p})$	7.9 ± 3.1	$(8.6 \pm 3.4 \pm 3.7) \times 10^{-5}$	585[7]	$(10.0 \pm 1.0) \times 10^{-5}$	[7, 8]
$\mathcal{B}(\chi_{c1} \to \pi^+\pi^-\pi^+\pi^-)$	254 ± 19	$(4.77 \pm 0.35 \pm 0.78) \times 10^{-3}$	72 ± 12	$(1.6 \pm 0.5) \times 10^{-2}$	[2]
$\mathcal{B}(\chi_{c2} \to \pi^+\pi^-\pi^+\pi^-)$	439 ± 21	$(10.14 \pm 0.49 \pm 1.59) \times 10^{-3}$	89 ± 12	$(2.2 \pm 0.5) \times 10^{-2}$	[2]
$\mathcal{B}(\chi_{c0} \to K^0_s K^0_s)$	53.8 ± 3.3	$(2.39 \pm 0.14 \pm 0.41) \times 10^{-3}$			
$\mathcal{B}(\chi_{c2} \to K^0_s K^0_s)$	9.1 ± 3.3	$(0.48 \pm 0.17 \pm 0.10) \times 10^{-3}$			
$\mathcal{B}(\chi_{c0} \to \pi^+\pi^-K^+K^-)$	567 ± 26	$(14.20 \pm 0.65 \pm 2.67) \times 10^{-3}$	83 ± 11	$(3.0 \pm 0.7) \times 10^{-2}$	[2]
$\mathcal{B}(\chi_{c1} \to \pi^+\pi^-K^+K^-)$	181 ± 15	$(4.58 \pm 0.37 \pm 0.87) \times 10^{-3}$	24 ± 7	$(9 \pm 4) \times 10^{-3}$	[2]
$\mathcal{B}(\chi_{c2} \to \pi^+\pi^-K^+K^-)$	252 ± 16	$(7.92 \pm 0.52 \pm 1.61) \times 10^{-3}$	47 ± 8	$(1.9 \pm 0.5) \times 10^{-2}$	[2]
$\mathcal{B}(\chi_{c0} \to \pi^+\pi^-p\bar{p})$	69.3 ± 9.9	$(1.60 \pm 0.23 \pm 0.39) \times 10^{-3}$	23 ± 6	$(5.0 \pm 2.0) \times 10^{-3}$	[2]
$\mathcal{B}(\chi_{c1} \to \pi^+\pi^-p\bar{p})$	16.9 ± 6.2	$(0.35 \pm 0.13 \pm 0.12) \times 10^{-3}$	6 ± 4	$(1.4 \pm 0.9) \times 10^{-3}$	[2]
$\mathcal{B}(\chi_{c2} \to \pi^+\pi^-p\bar{p})$	49.4 ± 8.0	$(1.28 \pm 0.21 \pm 0.32) \times 10^{-3}$	13 ± 5	$(3.3 \pm 1.3) \times 10^{-3}$	[2]
$\mathcal{B}(\chi_{c0} \to K^+K^-K^+K^-)$	64.4 ± 6.3	$(2.70 \pm 0.26 \pm 0.46) \times 10^{-3}$			
$\mathcal{B}(\chi_{c1} \to K^+K^-K^+K^-)$	9.2 ± 3.9	$(0.38 \pm 0.16 \pm 0.12) \times 10^{-3}$			
$\mathcal{B}(\chi_{c2} \to K^+K^-K^+K^-)$	37.9 ± 5.7	$(1.64 \pm 0.25 \pm 0.31) \times 10^{-3}$			
$\mathcal{B}(\chi_{c0} \to \phi\phi)$	6.6 ± 2.4	$(0.83 \pm 0.30 \pm 0.22) \times 10^{-3}$			
$\mathcal{B}(\chi_{c2} \to \phi\phi)$	12.5 ± 2.4	$(1.82 \pm 0.35 \pm 0.44) \times 10^{-3}$			
$\mathcal{B}(\chi_{c0} \to K^0_s K^+\pi^- + c.c.)$	< 10	$< 0.83 \times 10^{-3}$			
$\mathcal{B}(\chi_{c1} \to K^0_s K^+\pi^- + c.c.)$	31 ± 6	$(2.45 \pm 0.47 \pm 0.52) \times 10^{-3}$			
$\mathcal{B}(\chi_{c2} \to K^0_s K^+\pi^- + c.c.)$	< 14	$< 1.3 \times 10^{-3}$			
$\mathcal{B}(\chi_{c0} \to 3(\pi^+\pi^-))$	192 ± 16	$(12.62 \pm 1.02 \pm 2.35) \times 10^{-3}$	37 ± 8	$(1.5 \pm 0.5) \times 10^{-2}$	[2]
$\mathcal{B}(\chi_{c1} \to 3(\pi^+\pi^-))$	95 ± 11	$(5.76 \pm 0.67 \pm 0.94) \times 10^{-3}$	48 ± 15	$(2.2 \pm 0.8) \times 10^{-2}$	[2]
$\mathcal{B}(\chi_{c2} \to 3(\pi^+\pi^-))$	113 ± 12	$(9.13 \pm 0.95 \pm 1.58) \times 10^{-3}$	23 ± 15	$(1.2 \pm 0.8) \times 10^{-2}$	[2]

they distributed randomly in time, the 4C-fit and PARTID probability distributed the same as those of the events in χ_c mass region, the angular distribution of the fitted out photon not in some extra direction and the raw Shower Counter energy of the fitted out photons distributed around the fitted out energy, so seems more like signal than background. We also vary the cut position of the probabilities, PRB4C from 0.01 to 0.09, PRBID from 0.01 to 0.09, the signal still exist, but the background and the signal become smaller as the lower limits of the probabilities increase.

From above analyses and the result of Crystal Ball, we can draw the conclusion that the shoulder we see in the $\pi^+\pi^-K^+K^-$ and $3(\pi^+\pi^-)$ modes is indeed a signal, because it is seen in both inclusive gamma spectrum and two different hadronic decay modes.

In other channels except $\pi^+\pi^-K^+K^-$ and $3(\pi^+\pi^-)$ modes, the upper limits of η_c' production are estimated and are summarized in the table 2.

It is obvious that that $X(3594)$ results agree with the expectation of η_c' from η_c decays in some decay modes while deviate much in others(see table 3). This prevents us from regarding $X(3594)$ as the η_c' exact, but we can say that the characteristics of $X(3594)$, including its mass, width and decay modes, show that it is a strong candidate of the long searching η_c'.

References

[1] Particle Data Group, Phys. Rev. **D54**, PART I, 1996;

Table 2: Summary on $X(3594)$

$X(3594)$ decay mode	mass(MeV)	width(MeV)	Significance	Evts number	$\mathcal{B}(\psi' \to \gamma X(3594))\times$ $\mathcal{B}(X(3594) \to f)(\times 10^{-5})$
$\pi^+\pi^-K^+K^-$	3594 ± 8	< 10	3.1σ	31 ± 11	9.3 ± 6.7
$3(\pi^+\pi^-)$	3599 ± 13	< 9	2.1σ	10.5 ± 5.7	7.7 ± 5.9
$\pi^+\pi^-\pi^+\pi^-$					< 2.74
$K^+K^-K^+K^-$					< 1.04
$\pi^+\pi^-p\bar{p}$					< 1.70
$K_s^0K^+\pi^- + c.c.$					< 2.83
$p\bar{p}$					< 0.68

Table 3: Comparison between $X(3594)$ and η_c' expectation

$X(3594)$ decay mode	$\frac{\mathcal{B}(X(3594)\to f)}{\mathcal{B}(X(3594)\to\pi^+\pi^-K^+K^-)}$	$\frac{\mathcal{B}(\eta_c'\to f)}{\mathcal{B}(\eta_c'\to\pi^+\pi^-K^+K^-)}$
$\pi^+\pi^-K^+K^-$	1	1
$\pi^+\pi^-\pi^+\pi^-$	< 0.3	0.6 ± 0.3
$K^+K^-K^+K^-$	< 0.1	1.1 ± 0.7
$\pi^+\pi^-p\bar{p}$	< 0.2	< 0.6
$K_s^0K^+\pi^- + c.c.$	< 0.3	0.9 ± 0.4
$p\bar{p}$	< 0.07	0.06 ± 0.03
$3(\pi^+\pi^-)$	0.8 ± 0.8	–

[2] W.Tanenbaum *et al.*, Phys. Rev. **D17**, 1731(1978);

[3] C.Edwards *et al.*, Phys. Rev. Lett. **48**, 70(1982)

[4] T.A.Armstrong *et al.*, Phys. Rev. **D52**, 4839(1995);

[5] M. Baker *et al.*, Phys. Rev. **D51**, 1968(1995);
Yu-Qi Chen and R.J. Oakes, NUHEPTH-95-05, 1995;
S.N. Gupta *et al.*, Phys. Rev. **D49**, 1551(1994);

[6] K.T. Chao, Y.F. Gu and S.F. Tuan, Commun. Theor. Phys. **25**, 471(1996);

[7] T.A.Armstrong *et al.*, Phys. Rev. **D47**, 772(1993);
T.A.Armstrong *et al.*, Nucl. Phys. **B373**, 35(1992);
T.A.Armstrong *et al.*, Phys. Rev. Lett. **68**, 1468(1992);
T.A.Armstrong *et al.*, Phys. Rev. Lett. **69**, 2337(1992);
T.A.Armstrong *et al.*, Phys. Rev. **D52**, 4839(1995);

[8] C.Baglin *et al.*, Phys. Lett. **B172**. 455(1986);

[9] J.E.Gaiser *et al.*, Phys. Rev., **D34**, 711(1986);

[10] R. Brandelik *et al.*, Z. Phys. **C1**, 233(1979).